



## NRC Publications Archive Archives des publications du CNRC

### **Densely sulfophenylated segmented copoly(arylene ether sulfone) proton exchange membranes**

Li, Nanwen; Hwang, Doo Sung; Lee, So Young; Liu, Ying-Ling; Lee, Young Moo; Guiver, Michael D.

This publication could be one of several versions: author's original, accepted manuscript or the publisher's version. /  
La version de cette publication peut être l'une des suivantes : la version prépublication de l'auteur, la version  
acceptée du manuscrit ou la version de l'éditeur.

For the publisher's version, please access the DOI link below. / Pour consulter la version de l'éditeur, utilisez le lien  
DOI ci-dessous.

#### **Publisher's version / Version de l'éditeur:**

<https://doi.org/10.1021/ma200937w>

*Macromolecules*, 44, 12, pp. 4901-4910, 2011-05-24

#### **NRC Publications Record / Notice d'Archives des publications de CNRC:**

<https://nrc-publications.canada.ca/eng/view/object/?id=fe89b819-f2ad-4143-8a66-7544d7085659>

<https://publications-cnrc.canada.ca/fra/voir/objet/?id=fe89b819-f2ad-4143-8a66-7544d7085659>

Access and use of this website and the material on it are subject to the Terms and Conditions set forth at

<https://nrc-publications.canada.ca/eng/copyright>

READ THESE TERMS AND CONDITIONS CAREFULLY BEFORE USING THIS WEBSITE.

L'accès à ce site Web et l'utilisation de son contenu sont assujettis aux conditions présentées dans le site

<https://publications-cnrc.canada.ca/fra/droits>

LISEZ CES CONDITIONS ATTENTIVEMENT AVANT D'UTILISER CE SITE WEB.

**Questions?** Contact the NRC Publications Archive team at

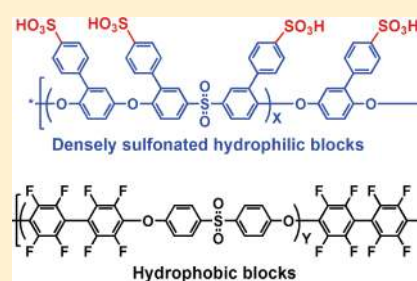
PublicationsArchive-ArchivesPublications@nrc-cnrc.gc.ca. If you wish to email the authors directly, please see the  
first page of the publication for their contact information.

**Vous avez des questions?** Nous pouvons vous aider. Pour communiquer directement avec un auteur, consultez la  
première page de la revue dans laquelle son article a été publié afin de trouver ses coordonnées. Si vous n'arrivez  
pas à les repérer, communiquez avec nous à PublicationsArchive-ArchivesPublications@nrc-cnrc.gc.ca.



Densely Sulfophenylated Segmented Copoly(arylene ether sulfone) Proton Exchange Membranes<sup>†</sup>Nanwen Li,<sup>‡</sup> Doo Sung Hwang,<sup>‡</sup> So Young Lee,<sup>§</sup> Ying-Ling Liu,<sup>||</sup> Young Moo Lee,<sup>\*,‡,§</sup> and Michael D. Guiver<sup>\*,‡,⊥</sup><sup>†</sup>WCU Department of Energy Engineering, College of Engineering, Hanyang University, Seoul 133-791, Republic of Korea<sup>§</sup>School of Chemical Engineering, College of Engineering, Hanyang University, Seoul 133-791, Republic of Korea<sup>||</sup>Department of Chemical Engineering, R&D Center for Membrane Technology, Chung Yuan Christian University, Chungli, Taoyuan 32023, Taiwan<sup>⊥</sup>Institute for Chemical Process and Environmental Technology, National Research Council, Ottawa, Ontario K1A 0R6, Canada

**ABSTRACT:** Segmented copoly(arylene ether sulfone) membranes having densely sulfonated pendent phenyl blocks were synthesized by the coupling reaction of phenoxide-terminated oligomers with bis(4-hydroxyphenyl) sulfone and decafluorobiphenyl (DFBP), followed by postpolymerization sulfonation of the blocks containing pendent phenyl substituents. The coupling reaction was conducted at relatively low temperature by utilizing highly reactive DFBP to prevent any possible trans-etherification that would randomize the hydrophilic–hydrophobic sequences. Segmented copolymer molecular weights were reasonably high, as determined by viscosity measurements. Postsulfonation occurred selectively on the pendent phenyl substituent to yield hydrophilic blocks that were highly sulfonated in regular sequence on the linked phenyl rings. The resulting polymers gave transparent, flexible, and tough membranes by solution casting. Morphological observation by transmission electron microscopy (TEM) and atomic force microscopy (AFM) showed that the high local concentration and regular sequence of pendent sulfonic acid groups within the hydrophilic blocks enhanced nanophase separation between the hydrophobic and hydrophilic blocks. A comparison of copolymers with similar ion exchange capacities (IECs) indicated that proton conductivity and water uptake were strongly influenced by the hydrophilic block sequence lengths. Proton conductivity and water uptake increased with increasing block length, even at low relative humidity (RH). The ionomer membrane with X20Y20 (X and Y refer to the number of hydrophilic and hydrophobic repeat units, respectively) and 1.82 mequiv/g of IEC had a proton conductivity of  $3.6 \times 10^{-2}$  S/cm at 80 °C and 50% RH, which is comparable to that of perfluorinated ionomer (Nafion) membrane ( $4.0 \times 10^{-2}$  S/cm).



## INTRODUCTION

Polymer electrolyte membrane fuel cells (PEMFCs) are promising energy conversion devices because of their high fuel utilization efficiency and environmentally clean operation.<sup>1–3</sup> Perfluorinated ionomers such as Nafion are the most widely used PEM materials in fuel cell applications due to their high proton conductivity and chemical stability, but well-known limitations such as high cost, high fuel crossover, restricted operation temperature, and humidity conditions prevent their widespread use in PEMFCs.<sup>4–6</sup> Acid-functionalized aromatic polymers have been investigated intensively over the past decade as alternative PEMs.<sup>7–9</sup> Despite these efforts, the performance of many hydrocarbon PEMs, especially proton conductivity under conditions of low relative humidity, is still inferior to that of perfluorinated PEMs. Consequently, the understanding of PEM properties that result from different polymer architectures is essential for the further improvement of hydrocarbon PEMs.

The proton conductivity of PEMs is usually closely related to several parameters such as acidity, number and position of ionic groups, main chain and/or side chain structures, composition and sequence of hydrophilic and hydrophobic components, and

membrane morphology.<sup>7,10,11</sup> Among these, acidity of ionic groups and membrane morphology appear to be crucial, and they are inter-related. Kreuer et al.<sup>12</sup> reported that typical sulfonated aromatic polymers are unable to form defined hydrophilic domains, as the rigid aromatic backbone prevents the formation of continuous conducting channels and ionic clustering from occurring. Thus, several approaches have been examined to improve proton conductivity under conditions of low humidity and high temperature.

One approach to enhance PEM performance is to induce phase separation between the hydrophilic sulfonic acid-containing regions and the hydrophobic polymer main chain, by positioning the sulfonic acid groups on side chains grafted onto the polymer main chain.<sup>13</sup> If the polymer architecture is such that it contains flexible pendent side chains linking the polymer main chain and the sulfonic acid groups, nanophase separation between hydrophilic and hydrophobic domains may be improved.<sup>14,15</sup> For example, Jannasch and co-workers reported PEMs prepared by

Received: April 23, 2011

Revised: May 13, 2011

Published: May 24, 2011

attaching flexible pendent sulfonated aromatic side chains to polysulfone, which showed proton conductivities of 11–32 mS/cm at 120 °C.<sup>14</sup> In previous work, we reported a series of pendant copolymers showing reasonable performance compared to Nafion membranes.<sup>16–18</sup>

Recently, efforts have been focused on the formation of poly(arylene ether) multiblock copolymers containing perfectly alternating hydrophilic and hydrophobic segments.<sup>19–22</sup> Ion-rich channels have been shown to form when the hydrophobic and hydrophilic domains of these multiblock copolymers nano-phase separate, allowing for higher conductivity, even under partially hydrated conditions.<sup>23</sup> McGrath et al.<sup>10</sup> reported multiblock copolymers, which were synthesized by a two-step polycondensation, with varying block lengths. For similar IEC values, the multiblock copolymers displayed higher conductivities at lower RH compared to similarly structured random copolymers. At the longer block lengths, this multiblock copolymer showed enhanced conductivity over the entire RH range when compared to Nafion 112. Membranes having a relatively low IEC of 0.95 mequiv/g had water uptake of 40%, but high proton conductivity of 80 mS/cm. Recently, densely sulfonated<sup>24–28</sup> or multiblock copolymers<sup>29–34</sup> have been attracting increasing attention because of the high contrast in polarity between the hydrophilic and hydrophobic units; this promotes the formation of hydrophilic–hydrophobic phase-separated structures. Bae et al.<sup>31</sup> have synthesized multiblock sulfonated poly(arylene ether sulfone ketone) (B-SPESK) containing highly sulfonated hydrophilic blocks. The B-SPESK membranes with IEC values of 1.62 mequiv/g had proton conductivity comparable to Nafion in the range of 20–90% RH and at 80 °C. A fuel cell was successfully operated with this membrane under conditions of 30% and 53% RH at 100 °C.

Segmented copolymers have also been synthesized for use as PEMs in fuel cells.<sup>35–37</sup> This technique involves the synthesis of one oligomeric block with difunctional end groups, which is then combined stoichiometrically with appropriate monomers, forming the other block in situ while the overall copolymer is being formed.<sup>38</sup> Although the multiblock copolymer structures produced by the segmented technique are less well-defined, this methodology has the great advantage of forming multiblock copolymers that can be synthesized more easily and in a shorter time, because there is no need to synthesize both oligomers separately and then couple them together.<sup>37</sup>

To the best of our knowledge, the combination of the three aforementioned features for PEM materials, that is, (1) segmented copolymers, (2) with densely sulfonated hydrophilic blocks, and (3) pendent phenylsulfonic acid groups, has never been reported so far. Herein, we report the preparation of segmented copoly(ether sulfone)s with densely sulfonated pendent phenyl sulfonic acid groups. The copolymers were prepared by the coupling reaction of corresponding hydroxyl-terminated pendent-phenyl oligomers with DFBP and bis(4-hydroxyphenyl) sulfone (BHPS), followed by postpolymerization sulfonation. These membranes address a combination of three aforementioned structural features that help to improve proton conduction, which are segmented polymer architecture, densely sulfonated blocks, and pendent sulfonic acid groups. In contrast with the present work, nearly all multiblock PEM structures reported to date do not have sulfonic acid groups that are substituted regularly along the block length. Selected PEM properties such as thermal and chemical stability, mechanical strength, water uptake behavior, and proton conductivity were investigated in detail.

## EXPERIMENTAL SECTION

**Materials.** Decafluorobiphenyl (DFBP) was obtained from Sigma-Aldrich and dried under vacuum at room temperature overnight. 3,3'-Diphenyl-4,4'-difluorodiphenyl sulfone (DPDFDPS) was synthesized according to a procedure reported elsewhere.<sup>18</sup> Bis(4-hydroxyphenyl) sulfone (BHPS) was purchased from Alfa Aesar and dried under vacuum at 80 °C for 24 h before use. 2-Phenylhydroquinone (PHQ) was obtained from Sigma-Aldrich and recrystallized from toluene. All other solvents and reagents (obtained from Sigma-Aldrich) were reagent grade and were used as received.

**Typical Synthesis of Hydroxyl-Terminated Oligomers (for X = 10).** PHQ (4.469 g, 22 mmol), DPDFDPS (8.219 g, 20 mmol), 1-methyl-2-pyrrolidinone (NMP, 50 mL), and toluene (20 mL) were stirred in a 100 mL round-bottomed flask, and the reaction mixture was heated with a Dean–Stark trap at 140 °C for 4 h and then at 165 °C for a further 20 h. The resulting slightly viscous mixture was poured dropwise into water. The recovered crude product was washed with deionized water and methanol several times and dried in a vacuum oven overnight.

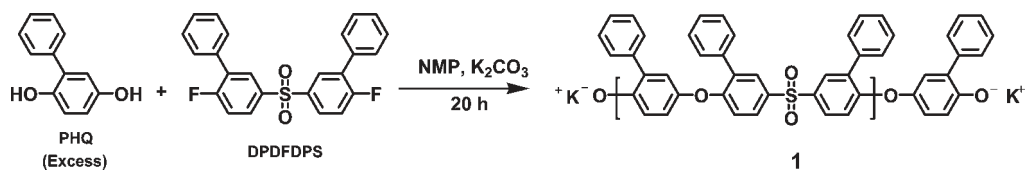
**Synthesis of Segmented Copolymers.** A sample copolymerization procedure was as follows (X10Y20): a three-neck, round-bottom flask, equipped with mechanical stirrer, Dean–Stark trap, condenser, and N<sub>2</sub> inlet, was loaded with the above hydroxyl-terminated hydrophilic oligomers ( $M_n = 5600$  g/mol, 1.1 g, 0.2 mmol), DFBP (1.4 g, 4.2 mmol), BHPS (1.0 g, 4 mmol), and NMP (15 mL). After dissolution of the reactants, K<sub>2</sub>CO<sub>3</sub> (0.69 g, 5 mmol) and cyclohexane (5 mL) were added to the reaction solution. The bath was heated to 80 °C, and the reaction was allowed to azeotrope water for 4 h. The cyclohexane was then drained from the system, and the bath temperature was increased to 85 °C where it was maintained for 6 h. The viscous solution was cooled and precipitated into water. The product was filtered and washed in deionized water at RT for 12 h and methanol for 12 h. It was dried at 80 °C in a vacuum oven overnight.

**Sulfonation of the Segmented Copolymer.** To a round-bottomed flask equipped with a dropping funnel, 1.0 g of segmented copolymer was charged. Then, dry dichloromethane (40 mL) was added into the flask, and the mixture was cooled to 5–10 °C. To the mixture was added dropwise a solution of chlorosulfonic acid (0.6 mL, 3 mmol) in dry dichloromethane (20 mL) at 5 °C. It was stirred vigorously at this temperature for 20–30 min until a dark brown product precipitated out of the solution. The precipitate was washed with water and ice several times and dried overnight under a vacuum at 80 °C for 10 h to give sulfonated segmented copolymers.

A solution of the obtained copolymer (1.0 g) in NMP (10 mL) was filtered and then cast onto a glass plate. Drying of the solution at 80 °C overnight gave a thick, transparent, tough film. The film was dried further in a vacuum oven at 100 °C for 20 h. The resulting membrane was treated with a 2 M aqueous solution of H<sub>2</sub>SO<sub>4</sub> for 24 h, washed with water several times, and dried at room temperature.

**Measurements.** <sup>1</sup>H NMR spectra were measured at 300 MHz on a Bruker AV 300 spectrometer using DMSO-*d*<sub>6</sub> or CDCl<sub>3</sub> as solvent. Ion-exchange capacities (IEC) of the membranes were determined by back-titration and <sup>1</sup>H NMR analysis. A weighed piece of membrane was equilibrated in a large excess of 0.5 M NaCl aqueous solution for 3 days. The HCl released by the ion exchange was titrated with standard 0.01 M NaOH solution. The reduced viscosities were determined on 0.5 g dL<sup>-1</sup> concentration of polymer in NMP or DMSO with an Ubbelohde capillary viscometer at 30 ± 0.1 °C. Tensile measurements were performed with a mechanical tester Instron-1211 instrument at a speed of 1 mm/min at room temperature (25 °C) and 50% relative humidity (RH). All the membranes were dried in vacuum at 100 °C for 10 h and equilibrated at 25 °C and 50% RH for at least 24 h before measurement. The thermogravimetric analyses (TGA) were obtained in nitrogen with a Perkin-Elmer TGA-2 thermogravimetric analyzer at a heating rate of

## Scheme 1. Synthesis of the Phenoxide-Terminated 1 with Controlled Molecular Weight



10 °C/min. The glass-transition temperatures ( $T_g$ ) were determined on a Seiko 220 DSC instrument at a heating rate of 20 °C/min under nitrogen protection.  $T_g$  is reported as the temperature at the middle of the thermal transition from the second heating scan. The molecular weights of polymers were determined by gel permeation chromatography (GPC) using a Waters 515 HPLC pump, coupled with a Waters 410 differential refractometer detector and a Waters 996 photodiode array detector. THF was used as the eluant and the  $\mu$ -Styragel columns were calibrated by polystyrene standards.

Membrane densities and IEC<sub>v</sub> (dry) were determined according to previously reported methods,<sup>39</sup> and the IEC<sub>v</sub> (wet) (mequiv/cm<sup>3</sup>) was then calculated based on membrane water uptake using the equation

$$\text{IEC}_v(\text{wet}) = \frac{\text{IEC}_w}{\frac{1}{\rho_{\text{polymer}}} + \frac{\text{WU}(\text{wt}\%)}{100 \times \rho_{\text{water}}}} \quad (1)$$

where IEC<sub>w</sub> is the gravimetric IEC (mequiv/g) and  $\rho$  (g/cm<sup>3</sup>) is the density.

The proton conductivity ( $\sigma$ , S cm<sup>-1</sup>) of each membrane coupon (size: 1 cm × 4 cm) was obtained using  $\sigma = d/L_s W_s R$  ( $d$  is the distance between reference electrodes, and  $L_s$  and  $W_s$  are the thickness and width of the membrane, respectively). The resistance value ( $R$ ) was measured over the frequency range from 100 mHz to 100 kHz by four-point probe alternating current (ac) impedance spectroscopy using an electrode system connected with an impedance/gain-phase analyzer (Solartron 1260) and an electrochemical interface (Solartron 1287, Farnborough Hampshire, ONR, UK). The membranes were sandwiched between two pairs of gold-plated electrodes. Conductivity measurements under fully hydrated conditions were carried out with the cell immersed in liquid water. Proton conductivity under partially hydrated conditions was performed at 80 °C. Membranes were equilibrated at different relative humidity for 2 h in a humidity–temperature oven before each measurement.

From the conductivity and density data, proton diffusion coefficients ( $D_o$ ) were calculated using the Nernst–Einstein equation

$$D_o = \frac{RT}{F_2} \frac{\sigma}{c(\text{H}^+)} \quad (2)$$

where  $R$  is gas constant,  $T$  is the absolute temperature (K),  $F$  is the Faraday constant, and  $c(\text{H}^+)$  is the concentration of proton charge carrier (mol/L).

AFM micrographs were recorded with a bioatomic force microscopy (Bio-AFM). AFM tapping-mode height profiles were acquired with a JPK Instruments AG multimode NanoWizard (Germany). The instrument was equipped with a NanoWizard scanner. For tapping-mode AFM, a commercial Si cantilever (TESP tip) of about 320 kHz resonant frequency from JPK was used.

For transmission electron microscopy (TEM) observations, the membranes were stained with lead ions by ion exchange of the sulfonic acid groups in 0.5 M lead acetate aqueous solution, rinsed with deionized water, and dried in vacuum oven for 12 h. The stained membranes were embedded in epoxy resin, sectioned to 70 nm thickness with a RMC MTX Ultra microtome, and placed on copper grids. Electron micrographs were

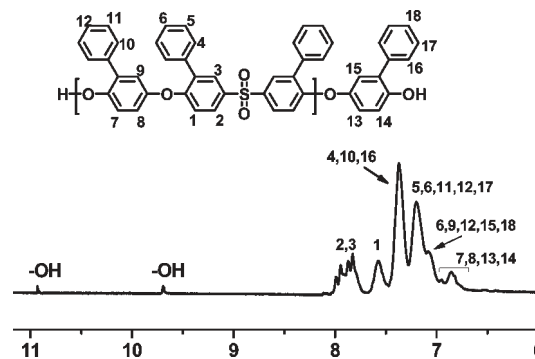


Figure 1. <sup>1</sup>H NMR spectrum of –OH-terminated oligomer 1 ( $X = 5$ ) acidified with dilute HCl.

taken with a Carl Zeiss LIBRA 120 energy-filtering transmission electron microscope using an accelerating voltage of 120 kV.

## RESULTS AND DISCUSSION

**Synthesis and Characterization of OH-Terminated Oligomers.** The OH-terminated oligomers having a high concentration of pendent phenyl groups were synthesized as shown in Scheme 1. The monomer composition was adjusted to provide oligomers with three values for the degree of polymerization: 5, 10 and 20.

After polymerization and site-specific sulfonation of the pendent phenyl groups, the uniformly spaced pendent sulfonic acid groups within the hydrophilic blocks was expected to provide a dense continuity of conducting groups, resulting in enhanced phase separation between and hydrophilic and hydrophobic blocks. For example, 30 pendent sulfonic acid groups are located with continuous uniform spacing in the  $X = 10$  hydrophilic block and 60 conducting groups for  $X = 20$ . The oligomerization reaction was conducted in NMP under typical nucleophilic substitution polycondensation conditions using potassium carbonate as a base, and the products were characterized by GPC analyses. Unlike many previously reported block copolymers, in which <sup>1</sup>H NMR was used for end-group analysis to confirm the  $M_n$  of the oligomers, the chemical shift and integration of the end-group aromatic proton signals are difficult to discern for these phenoxide-terminated oligomers (Figure 1). However, the end-group –OH signals become apparent after treating the oligomers with aqueous HCl. As shown in Figure 1, the signals at 9.72 and 10.85 ppm can be contributed the chemical shift of –OH protons in the end group.  $M_n$  was determined by comparative integration of –OH to main chain signals. The  $X$  values thus calculated by <sup>1</sup>H NMR were 7.5 for  $X = 5$  and 13.2 for  $X = 10$ . The length for the  $X = 20$  oligomer could not be determined by this method.

Molecular weight distributions ( $M_w/M_n$ ), measured by GPC in THF, were in the range of 1.6–2.0, which were typical of polycondensation (Table 1). The experimental  $X$  values calculated from GPC  $M_n$  were 7.2 ( $X = 5$ ), 12.6 ( $X = 10$ ), and 21.2 ( $X = 20$ ), which were similar to those obtained by  $^1\text{H NMR}$ . These values were somewhat higher than those expected from the monomer feed ratio, especially for the short length oligomers. For the subsequent segmented copolymerization,  $X$  values obtained by GPC data were used to balance the stoichiometry.

**Synthesis and Sulfonation of Segmented Copolymers.** Segmented copolymerization of the oligomers with DFBP and BHPS monomers was conducted in the presence of potassium carbonate (Scheme 2).

Simultaneous formation of the hydrophobic segments and the block copolymer eliminated the need to synthesize and isolate a separate hydrophobic block before coupling it to the hydrophilic block. The highly reactive DFBP monomer allowed for mild reaction temperatures (85 °C) to be used during copolymerization,

which would help to suppress any randomization that could occur by possible ether–ether interchange. To achieve high molecular weight, it was important to ensure that the overall ratio of phenoxide to para-F end-groups was 1:1. An excess of phenoxide groups is disadvantageous because the ortho-fluorines on the DFBP are also able to react with the excess phenoxide groups, resulting in a cross-linked network. A short polymerization time of 6 h at 85 °C was sufficient to give highly viscous solutions of high molecular weight products without cross-linking. The copolymers were obtained as fibers, which were soluble in many organic solvents such as chloroform, DMF, DMSO, DMAc, and NMP. Comparison of the  $^1\text{H NMR}$  spectra with those of the parent OH-terminated oligomers **1** revealed that the –OH protons were absent in the resulting segmented copolymers, and new signals appeared at 8.01 and 7.52 ppm, corresponding to BHPS protons. As shown in Table 2, the obtained segmented copolymers **2** (nonsulfonated) displayed high reduced viscosity values in the range 0.68–0.85 dL/g, which, when considered with other measurements such as AFM, indicated the formation of segmented copolymers. The  $Y$  values in **2** were experimentally determined from the  $X$  values of **1** and  $^1\text{H NMR}$  spectrum of **2** and are summarized in Table 2. These experimental  $Y$  values are closely comparable to the ones expected from the comonomer feed composition.

The prepared segmented copolymers were sulfonated with chlorosulfonic acid in dichloromethane solution. Using the experimental  $X$  and  $Y$  values as a reference, a 5-fold molar excess of chlorosulfonic acid was necessary for complete sulfonation of the pendent phenyl substituents of **2**. The degree of sulfonation and experimental IEC values were determined by back-titration. Initially, sulfonation of **2** at 5 wt % concentration was performed

**Table 1.** Molecular Weight of Hydroxyl-Terminated Telechelic Oligomers

$X^a$	$\eta^b$	$X^c$	$M_n \times 10^{-3}{}^d$	$M_w \times 10^{-3}{}^d$	$M_w/M_n^d$	$X^d$
5	0.15	7.5	4.2	6.7	1.6	7.2
10	0.20	13.2	7.2	14.4	2.0	12.6
20	0.29		11.9	24.1	2.0	21.2

<sup>a</sup> Calculated value from the feed monomer ratio. <sup>b</sup> Measured in NMP with 0.5 g/L at 25 °C. <sup>c</sup> Determined by  $^1\text{H NMR}$  spectra. <sup>d</sup> Determined by GPC in THF.

**Scheme 2.** Synthesis of the Segmented Sulfonated Copolymers **3**

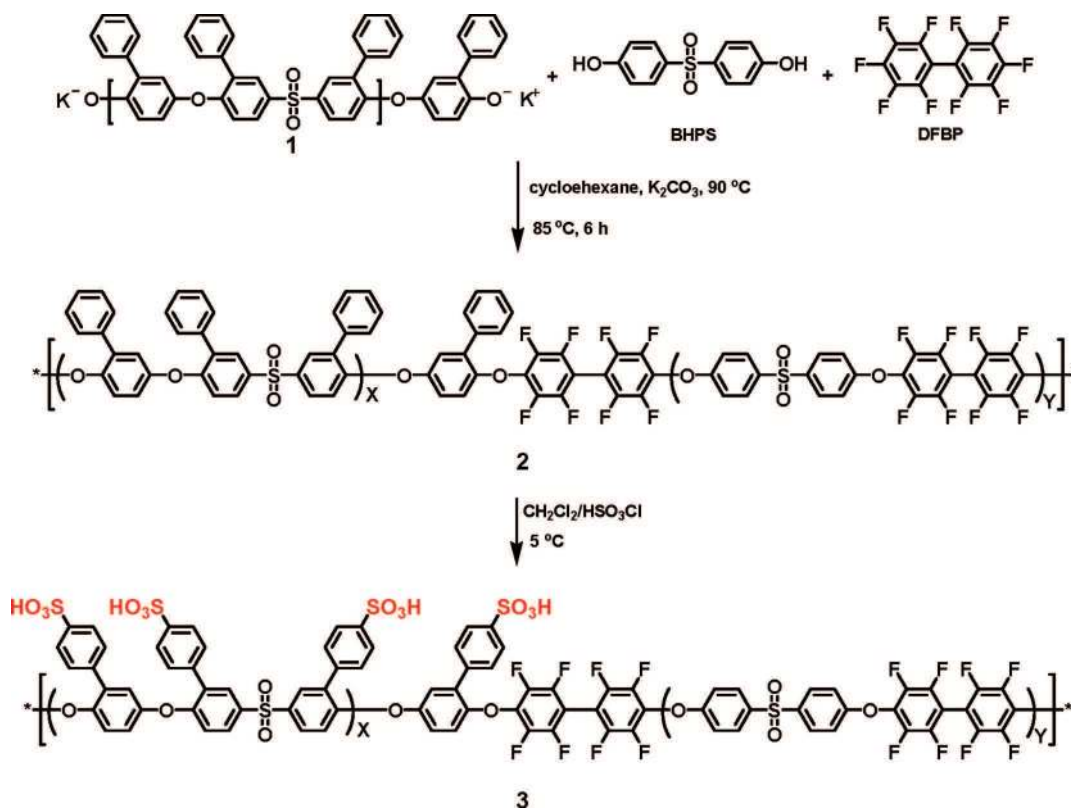


Table 2. IEC, Viscosity, and Thermal Stability of the Segmented Copolymer 3 Membranes

expected XY	experimental XY	$\eta^d$	sulfonation time (min)	IEC <sup>b</sup>	IEC <sup>c</sup>	degree of sulfonation	$\eta^d$	$T_g$ (°C)	$T_{d(\text{onset})}$ (°C)
X5Y15	X7Y25	0.69	30	1.12	1.03	100	1.25	223	287
X5Y10	X7Y18	0.78	30	1.42	1.41	100	1.36	223	279
X5Y7	X7Y12	0.82	25	1.74	1.60	90	1.22	225	265
X10Y30	X13Y52	0.75	30	1.01	1.00	100	1.25	225	291
X10Y25	X13Y40	0.85	30	1.21	1.20	100	1.28	224	285
X10Y20	X13Y29	0.76	30	1.52	1.46	100	1.23	227	278
X20Y60	X21Y75	0.68	30	1.03	0.98	100	1.15	224	292
X20Y40	X21Y48	0.81	25	1.53	1.49	100	1.31	225	287
X20Y30	X21Y37	0.73	20	1.76	1.63	90	1.25	225	268
X20Y20	X21Y28	0.68	20	2.06	1.82	86	1.34	227	266

<sup>a</sup> Before sulfonation, measured in NMP with 0.5 g/L at 30 °C. <sup>b</sup> Target IEC values. <sup>c</sup> Estimated by back-titration. <sup>d</sup> After sulfonation, measured in NMP with 0.5 g/L at 30 °C.

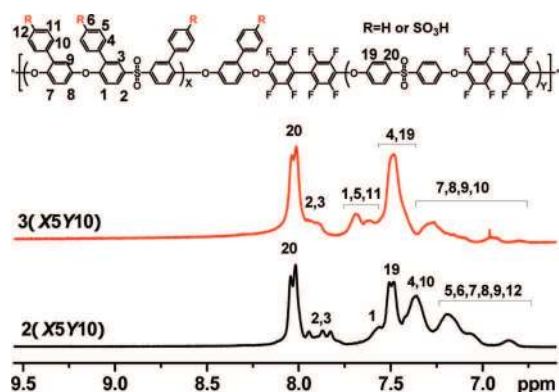


Figure 2. Comparative  $^1\text{H}$  NMR spectra of and nonsulfonated (2) and sulfonated (3) segmented copolymers X5Y10.

using 10 vol %  $\text{HSO}_3\text{Cl}$  in dichloromethane at room temperature. Although a low IEC value segmented copolymer could be achieved in a short time (about 25 min), the reaction did not give a sulfonated copolymer with a high IEC value; only an insoluble gel resulted. It has been reported that strong sulfonation reagents such as chlorosulfonic acid have a tendency to cause side reactions, including cross-linking and cleavage of polymer chain.<sup>40,41</sup> Therefore, reduced reaction temperatures and lower polymer and  $\text{HSO}_3\text{Cl}$  concentrations were investigated to suppress cross-linking. Even under milder conditions, sulfonation reaction times that extended beyond 30 min also resulted in gel formation. The degree of sulfonation was determined by titration. As shown in Table 2, a high degree of sulfonation was achieved. Most of the copolymers 2 could be sulfonated completely within a 30 min reaction time, and the experimental IEC values were consistent with those expected from the comonomer feed ratios. However, even these sulfonation conditions for preparing copolymers with high IEC and long block lengths also resulted in gel formation. Hence, a shorter sulfonation time (20 min) was required to avoid cross-linking for the X20Y30 and X20Y20 segmented copolymers, which had a degree of sulfonation of 90% and 86%, respectively. Thus, the experimental IEC of the 3 copolymers ranged from 0.98 to 1.82 mequiv/g.

Figure 2 shows a comparison of the  $^1\text{H}$  NMR spectra of nonsulfonated and sulfonated segmented X5Y10 copolymer 2. Comparison of the spectral signals reveals that the nonsulfonated pendent phenyl protons (H4, H10) at 7.38 ppm shift to 7.52 ppm

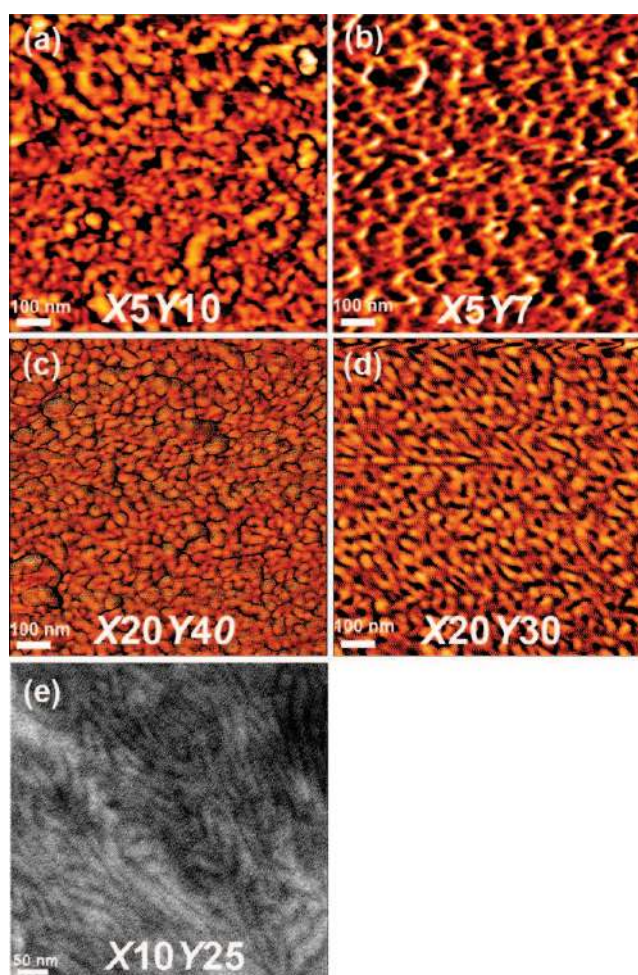


Figure 3. AFM image of 3 membranes (a–d) and TEM image of 3(X10Y25, IEC = 1.20 mequiv/g) membrane (e).

(H4) and 7.27 ppm (H10) after the sulfonation reaction, while other aromatic protons (H19, H20) remain, along with new signals 7.71 ppm assigned to the sulfonated pendent phenyl groups. Here, it is very difficult to reliably determine the experimental IEC values by  $^1\text{H}$  NMR because of overlapping of spectral signals. There was no evidence of chain degradation occurring under these conditions, as indicated by viscosity measurements and the

Table 3. Various IEC, Water Uptake, Swelling Ratio, and Proton Conductivities of 3 Membranes

XY	density	IEC <sub>w</sub>	IEC <sub>v</sub>		WU (wt %)		swelling ratio		conductivity (mS/cm)	
			dry	wet <sup>a</sup>	20 °C	80 °C	20 °C	80 °C	in water	50 RH%
XSY15	1.36	1.03	1.40	1.17	14.5	17.7	0.02	0.03	50	7
XSY10	1.43	1.41	2.02	1.44	28.2	34.3	0.05	0.05	92	10
XSY7	1.52	1.60	2.43	1.42	46.6	80.8	0.08	0.10	132	18
X10Y30	1.37	1.00	1.37	1.11	17.2	23.7	0.03	0.04	60	10
X10Y25	1.39	1.20	1.68	1.27	23.5	33.5	0.03	0.05	81	12
X10Y20	1.45	1.46	2.12	1.38	36.8	53.4	0.07	0.10	122	24
X20Y60	1.38	0.98	1.35	1.05	20.3	29.9	0.03	0.05	92	16
X20Y40	1.44	1.49	2.14	1.29	45.5	100.5	0.07	0.12	151	30
X20Y30	1.48	1.63	2.41	1.25	62.6	147.6	0.08	0.15	172	32
X20Y20	1.54	1.82	2.80	1.23	82.9	198.7	0.10	0.20	194	36
Nafion	1.98	0.90	1.78	1.29	19.0	28.6	0.12	0.19	90	40

mechanical properties of the sulfonated polymer films. The sulfonated copolymers **3** were soluble in DMSO, DMAc, and NMP and gave transparent and flexible membranes by solution casting.

#### Morphological Structures of Segmented **3** Membranes.

The tapping mode phase image of the copolymer **3**(X20Y40) and **3**(X20Y30) membranes was recorded under ambient conditions on  $1\ \mu\text{m} \times 1\ \mu\text{m}$  size scales to investigate its surface hydrophilic/hydrophobic morphology (Figure 3). The dark and bright regions correspond to the soft structure of the hydrophilic block sequence with sulfonic acid groups containing water and the hard structure of the hydrophobic block sequence, respectively. As can be seen in Figures 3a–d, the phase surface image exhibits clear hydrophilic/hydrophobic phase separation with an interconnected hydrophilic network of small ionic clusters, which is the result of the segmented structure in combination with the densely populated sulfophenylated groups. The interconnectivity of ionic clusters appears to be more pronounced for the longer hydrophilic block membranes (X20Y40 and X20Y30), which exhibit well-connected hydrophilic domains (Figures 3c,d). A similar morphology is also observed in Figure 3e, which is the cross-sectional transmission electron microscopic (TEM) image of the **3**(X10Y25) membrane showing dark and bright regions, corresponding to the hydrophilic (lead-ion-exchanged sulfonic acid groups) and hydrophobic domains, respectively. The hydrophilic domains (5–10 nm width) are interconnected, which presumably function as ionic channels in the thickness direction. These morphological considerations will be further discussed below in consideration of the water uptake and proton conductivity behavior.

#### Water Uptake and Dimensional Change of **3** Membranes.

Table 3 lists the water uptake of copolymer **3** membranes at 20 and 80 °C in water, in comparison with Nafion 112. As expected, higher IEC membranes absorbed more water due to the increased hydrophilicity. The highest water uptake were 82.9% at 20 °C in water for the highest IEC<sub>w</sub> membranes **3**(X20Y20) (IEC<sub>w</sub> = 1.82 mequiv/g), which was much higher than that of Nafion membrane. In addition to the impact of IEC<sub>w</sub>, the water uptake behavior of the segmented copolymers was also strongly influenced by hydrophilic block lengths. Specifically, the water uptake values for the segmented copolymers with similar IECs increased with increasing block length. For example, while the **3**(XSY15), **3**(X10Y30), and **3**(X20Y60) copolymers have very similar IEC<sub>w</sub> values of around 1.0 mequiv/g, the water uptake

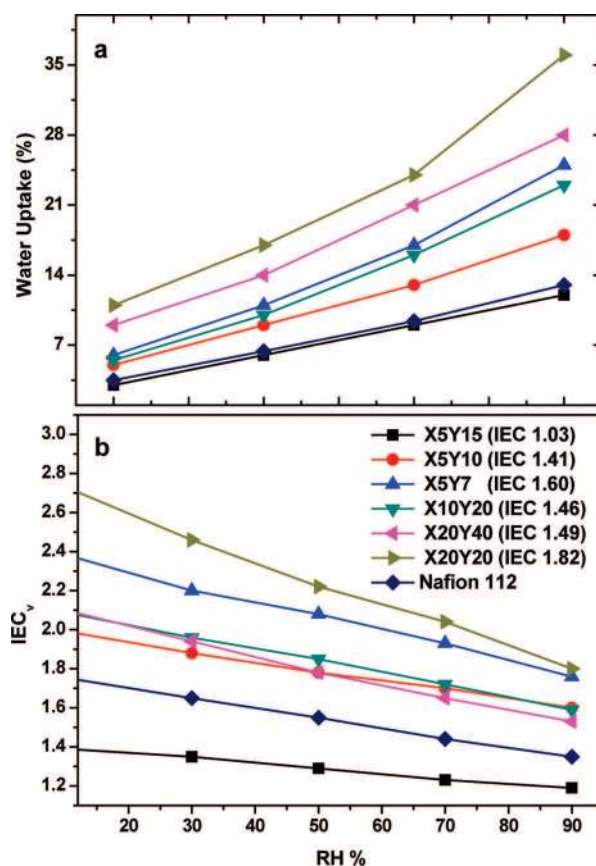


Figure 4. Water uptake (a) and volumetric IEC<sub>v</sub> (b) of selected **3** and Nafion 112 membranes as a function of relative humidity (RH) at 80 °C.

increased from 14.5% for the **3**(XSY15) to 20.3% for **3**(X20Y60). This result is consistent with the reported behavior of multiblock copolymers.<sup>11,19,21</sup>

A similar tendency was observed for the water uptake of segmented **3** membranes at low relative humidity (Figure 4a), as shown by the comparison of **3**(X20Y40) (IEC = 1.49 mequiv/g) and **3**(XSY10) (IEC = 1.41 mequiv/g). Moreover, temperature has a stronger influence on water uptake of **3** membranes with long hydrophilic blocks, as shown in Table 3. Thus, the membranes **3**(X20Y40) and **3**(X20Y20) absorbed excessive amounts

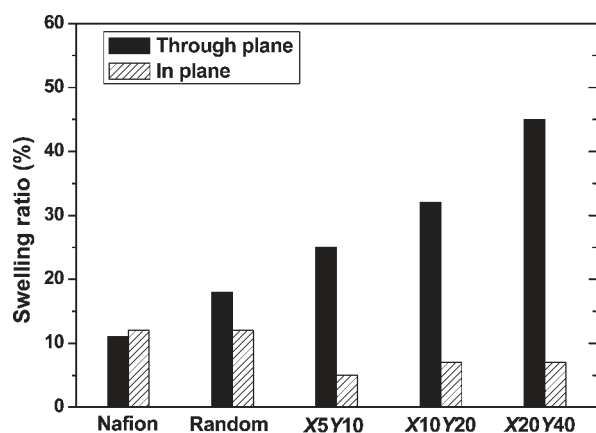


Figure 5. Comparison of dimensional swelling data for segmented 3, random (IEC = 1.64 mequiv/g),<sup>18</sup> and Nafion 112 membranes at 20 °C in water.

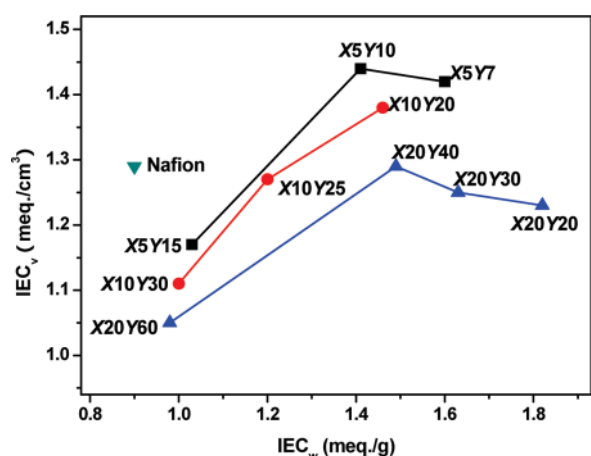


Figure 6. Volumetric IEC<sub>v</sub> (wet) in water at RT as a function of gravimetric IEC<sub>w</sub>.

of water, and their mechanic properties declined at 80 °C in water.

Dimensional stability of segmented copolymer membranes showed anisotropic swelling behavior with larger dimensional change in the through-plane direction than in the in-plane direction. For example, 3(X5Y10) showed 5% swelling ratio in the in-plane direction at room temperature in water, whereas the through-plane (thickness) swelling was 25%. Other samples such as 3(X10Y30) and 3(X20Y20) showed a similar tendency, which was in good accordance with the reported behavior of multiblock sulfonated copolymers.<sup>11,19,21</sup> Even at elevated temperature (80 °C), the segmented 3 membranes maintained a low swelling ratio in the in-plane direction compared to Nafion (Table 3). Although all the segmented copolymers showed similar in-plane swelling, the through-plane swelling increased with block length, as shown in Figure 5. The increase in water uptake and through-plane swelling with increasing block length may suggest the formation of ordered hydrophilic domains within the copolymer. The result was supported by the AFM and TEM results.

Volumetric IEC (IEC<sub>v</sub>, mequiv/cm<sup>3</sup>), which is defined as the molar concentration of sulfonic acid groups per unit volume containing absorbed water, is a useful parameter for the detailed comparison of the water uptake among the membranes. The

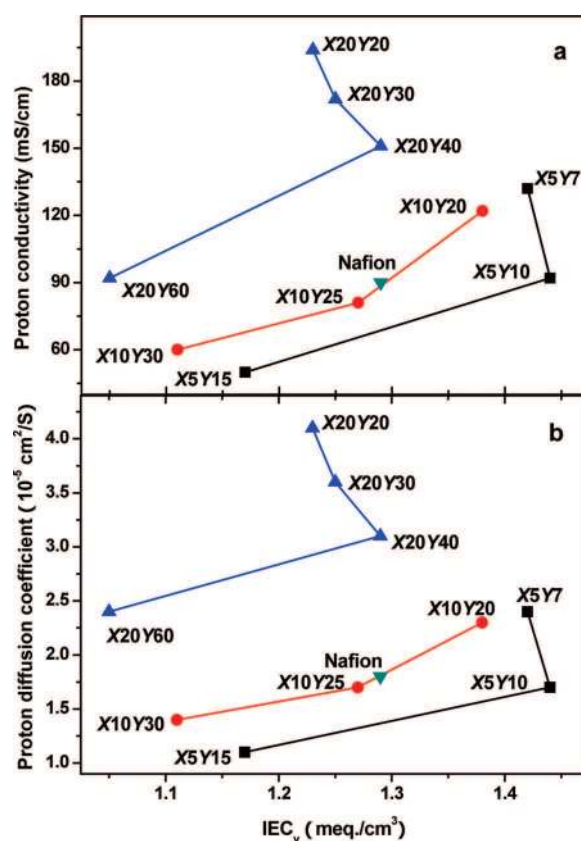


Figure 7. Proton conductivity (a) and proton diffusion coefficient (b) at 20 °C in water as a function of volumetric IEC<sub>v</sub> (wet).

IEC<sub>v</sub> (wet) reflects the concentration of ions within the polymer matrix under hydrated conditions. Usually, the IEC<sub>v</sub> (wet) of membranes increases with increasing IEC<sub>w</sub>. For example, the IEC<sub>v</sub> (wet) of copolymer 3 membranes with the block length of 10 increased from 1.11 to 1.38 mequiv/cm<sup>3</sup> as IEC<sub>w</sub> increased from 1.00 to 1.46 mequiv/g. However, high IEC<sub>w</sub> values result in high water uptake as discussed above; thus, the membranes shown decreased IEC<sub>v</sub>, as shown in Figure 6. For example, the 3(X20Y20) membranes with an IEC<sub>w</sub> of 1.82 mequiv/g showed an IEC<sub>v</sub> (wet) of 1.23 mequiv/cm<sup>3</sup>, which is lower than that of membrane 3(X5Y10) (IEC<sub>v</sub> = 1.44 mequiv/cm<sup>3</sup>, IEC<sub>w</sub> = 1.41 mequiv/g) (Figure 6).

For the high IEC<sub>w</sub> membranes, the high sulfonic acid group concentration results in excessive swelling and dilution of the ion concentration after equilibration with water. Therefore, the copolymer 3 membranes with longer block lengths are located on the lower area of Figure 6, which indicates that they have low IEC<sub>v</sub> (wet) because of their high water uptake.

The IEC<sub>v</sub> (wet) is plotted as a function of relative humidity at 80 °C in Figure 4b. The IEC<sub>v</sub> (wet) values became lower with increasing humidity due to increased water volume per sulfonic acid within the polymer matrix.

The 3(X5Y15) membranes had lower IEC<sub>v</sub> (wet) values compared with Nafion throughout a wide range of relative humidity, despite having similar water uptake and IEC<sub>w</sub> values because of differences in density (1.98 g/cm<sup>3</sup> for Nafion and 1.36 g/cm<sup>3</sup> for 3(X5Y15)). The other copolymer 3 membranes had higher IEC<sub>v</sub> than Nafion (Figure 4b). Another observation is that high IEC<sub>w</sub> or longer block length membranes have a slightly



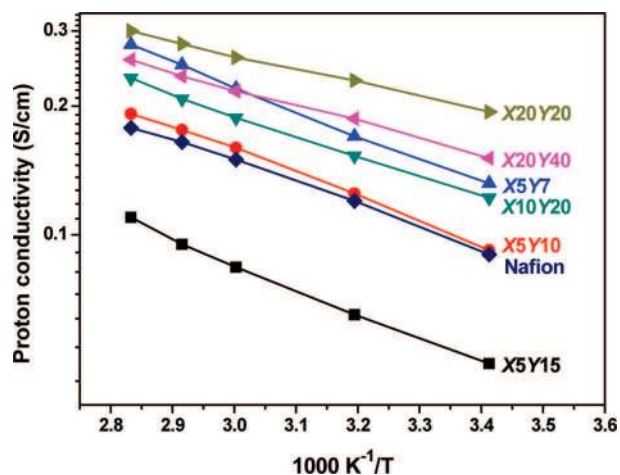


**Figure 8.** Proton conductivity of selected 3 and Nafion 112 membranes in water as a function of temperature.

higher humidity dependence on  $IEC_v(\text{wet})$ , as shown in Figure 4b, which can be attributed to a higher degree of water. The 3(X20Y40), for example, showed a higher slope than that of X5Y10 membrane.

**Proton Conductivity.** Proton conductivity values for the segmented copolymer membranes in liquid water at 20 °C are listed in Table 3. For random copolymers, proton conductivity normally scales with ion exchange capacity. For the segmented copolymers, an increase in conductivity values with  $IEC_w$  was also observed. Similar to the water uptake, the higher IEC membranes showed higher proton conductivity, as listed in Table 3. Most of the copolymer 3 membranes showed comparable or higher proton conductivity than Nafion membranes. The effect of block length is also consistent with the water uptake, in which the hydration of copolymer 3 membranes with high  $IEC_w$  values resulted in excessive swelling and dilution of the ion concentration, thus reduced  $IEC_v(\text{wet})$ . This is observed in Figure 7a, whereby the slope of the curves reverses direction due to reduced  $IEC_v(\text{wet})$ . As shown in Figure 7a, copolymer 3 membranes with longer block length showed higher proton conductivity. For example, the 3(X20Y60) membranes ( $IEC = 0.98$  mequiv/g) having longer blocks length have a similar IEC value with the 3(X5Y15) membrane ( $IEC = 1.03$  mequiv/g) but showed higher proton conductivity.

Figure 7b shows the proton diffusion coefficients ( $D_o$ ) through the copolymer 3 membranes in water, which were estimated from the proton conductivity (Figure 7a) and the  $IEC_v(\text{wet})$ . The membranes with short block length share similar proton diffusion coefficients with Nafion only when the  $IEC_v$  is high. Long block lengths (X20) lead to higher  $D_o$  values, shown in the upper area in the Figure 7b, than the shorter ones (X5 and X10) and Nafion. It is assumed that the segmented densely sulfophenylated copolymer structure influences the size and shape of the hydrophilic ionic domains, through which proton transport occurs, as confirmed by image analyses in Figure 3. The hydrophilic ionic domains result in high  $D_o$  values, and thus high proton conductivities of the copolymer 3 membranes, as shown in Figure 7a. In addition, the  $D_o$  values obtained for the present membranes were higher than those of our previous random copolymer membranes.<sup>18</sup> The results are congruent with the morphological data and validate our strategy of densely sulfophenylated segmented copolymer architecture to obtain highly proton conductive membranes.

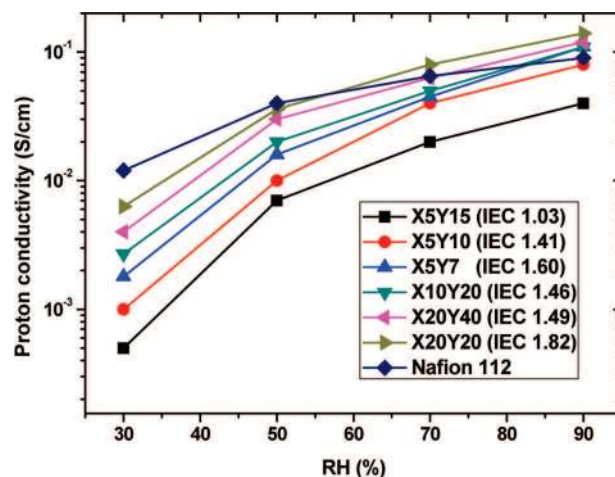


**Figure 9.** Dependence of proton conductivity on RH of Nafion 112 and selected 3 membranes at 80 °C.

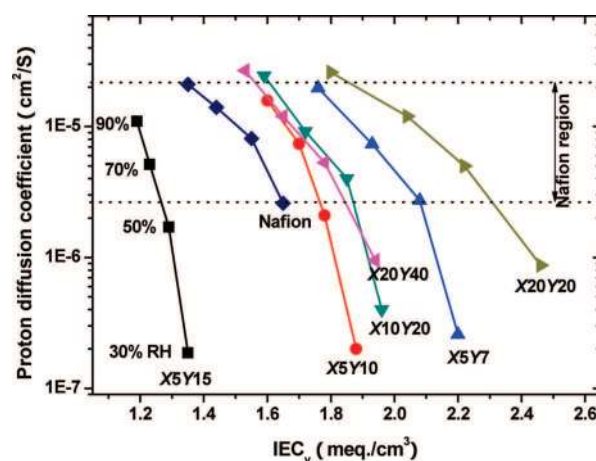


**Figure 10.** Proton diffusion coefficients of selected 3 and Nafion 112 membranes as a function of volumetric  $IEC_v$  at 80 °C.

In addition, the proton conductivities over the 20–100 °C range in water are shown in Figure 8. The segmented 3 membranes exhibit qualitative increases in conductivity with temperature as shown in the Arrhenius plot. Higher temperatures increase the conductivity due to the enhanced charge transport. The proton conductivity displays a remarkably stable behavior, with values above  $1 \times 10^{-1}$  S cm<sup>-1</sup> even at 80 °C. However, the copolymer 3 membranes having long hydrophilic blocks displayed a relatively low slope value; compare 3(X5Y7) and 3(X20Y40). The results indicated that long hydrophilic blocks decreased the barriers for proton transport. This behavior would be more obvious for the proton conductivity at low humidity, as shown below.

The humidity dependence of proton conductivity was measured for the copolymer 3 and Nafion 112 membranes at 80 °C. As can be seen in Figure 9, the membranes having  $IEC > 1.45$  mequiv/g ( $(1.1–1.5) \times 10^{-1}$  S/cm) show higher proton conductivity than that of Nafion 112 ( $0.9 \times 10^{-1}$  S/cm) at 90% RH. Although the proton conductivity is more dependent on relative humidity than that of Nafion 112, high proton conductivity comparable to Nafion 112 is achieved for some of the segmented copolymer membranes at 50% RH, which is attributable to their

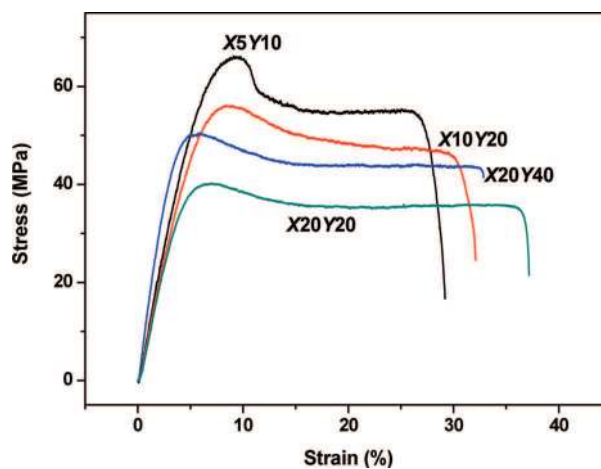
**Table 4. Mechanical Properties of 3 Membranes at 25 °C and 50% RH**

expected XY	IEC <sub>w</sub>	maximum stress (MPa)	Young's modulus (GPa)	elongation at break (%)
XSY15	1.03	68.2	1.30	32.2
XSY10	1.41	63.9	1.21	28.9
XSY7	1.60	54.7	1.17	37.2
X10Y30	1.00	65.3	1.26	30.5
X10Y25	1.20	59.6	1.31	28.1
X10Y20	1.46	54.5	1.12	32.2
X20Y60	0.98	59.2	1.23	27.4
X20Y40	1.49	48.5	1.03	34.7
X20Y30	1.63	43.7	0.98	35.6
X20Y20	1.82	39.4	0.91	38.2

well-connected ionic channels seen in the AFM and TEM results. Especially, proton conductivity of the 3(X20Y20) membrane at 50% RH ( $3.6 \times 10^{-2}$  S/cm) is closely similar to that of Nafion 112 ( $4.0 \times 10^{-2}$  S/cm) and still has a conductivity of  $6.3 \times 10^{-3}$  S/cm at 30% RH. The segmented copolymer 3 membranes with longer hydrophilic blocks exhibited better proton conductivity not only in liquid water, but also at low relative humidity.

Figure 10 compares the proton diffusion coefficients ( $D_{\sigma}$ ) as a function of IEC<sub>v</sub>. The Nafion region for  $D_{\sigma}$  is from  $2.68 \times 10^{-5}$  to  $2.56 \times 10^{-6}$  cm<sup>2</sup>/s, which is narrower than that of the 3 membranes. The wider range of  $D_{\sigma}$  for the 3 membranes implies that they are more dependent on relative humidity, in common with most aromatic ionomers.<sup>11,18</sup> At 90% RH, IEC<sub>v</sub> higher than 1.5 mequiv/cm<sup>3</sup> was required for the 3 membranes in order to have comparable  $D_{\sigma}$  to that of Nafion, since the lower  $D_{\sigma}$  of 3 could be compensated by higher IEC<sub>v</sub>. However, this was not the case at 30% RH since the differences in  $D_{\sigma}$  was too large to be compensated by IEC<sub>v</sub>. A general trend of the dependency of  $D_{\sigma}$  on the block length was obtained. The 3(X20Y40) membranes showed higher  $D_{\sigma}$  than that of 3(X10Y20), in spite of the former's lower IEC<sub>v</sub>, which is consistent with the finding that 3 membranes having longer block lengths had higher proton conductivity.

**Mechanical and Thermal Properties.** The mechanical properties of the polymers are listed in Table 4. For the sulfonated polymers in the dry state, the membranes demonstrated mechanical properties with tensile stresses of 39.4–68.2 MPa, Young's moduli of 0.91–1.31 GPa, and elongation at break values of 27.4–38.2%. Compared with the data of Nafion, with tensile stress of 38 MPa, Young's modulus of 0.18 GPa, and elongation at break of 301% measured under the same testing conditions,<sup>18</sup> the segmented copolymer materials showed higher tensile strength and lower elongation than Nafion. In addition, the segmented copolymers showed hardening after maximum stress (Figure 11), which implies that molecular rearrangement during stretching occurred. The block length had also some impact on the mechanical properties, with the general trend of lower Young's modulus for longer block length membranes. For example, 3(X20Y60) and 3(X20Y40) membranes showed lower stress at break point and lower Young's modulus than 3(XSY15) and 3(XSY10), respectively, which have similar IEC but shorter block length. The results are reasonable, taking higher water absorbability of long block length membranes into account. The developed hydrophilic aggregates in long block length membranes segregate

**Figure 11.** Stress vs strain curves of selected 3 membranes at room temperature and 50% RH.

hydrophobic blocks and consequently cause weaker physical interactions between hydrophobic blocks and lower mechanical strength of the membranes.

The thermal stability of sulfonated 3 membranes was investigated by TGA. There was no weight loss up to 200 °C because all the samples were preheated at 150 °C for 20 min to remove absorbed water. No obvious degradation could be observed until 250 °C (Table 2), which is possibly associated with the degradation of the sulfonic acid groups. Furthermore, only one transition temperature was observed in the DSC curves before the decomposition temperature, which indicated their amorphous nature. As shown in Table 2, the  $T_g$  values of the copolymer 3 membranes were in the range of 223–227 °C which were lower than the decomposition temperature (about 250 °C). The high thermal stability and moderate  $T_g$  values present the possibility of preparing membrane electrode assemblies (MEA) by hot pressing. Unlike the previous series of analogous random copolymers,<sup>18</sup> in which the high IEC value induced higher  $T_g$ , the IEC values of the present segmented copolymers was less likely to affect the  $T_g$ .

## CONCLUSIONS

Three structural approaches have been combined to produce new polymer architecture for efficient proton conduction: (a) segmented copolymer structure, (b) densely and uniformly sulfonated blocks, and (c) pendent phenyl sulfonic acid groups (sulfophenylated). The densely sulfonated segmented copoly(arylene ether sulfone)s were synthesized by the coupling reaction of hydroxyl-terminated poly(arylene ether sulfone) oligomer having a uniform and regular distribution pendent phenyl groups, with DFBP, at moderate temperature, followed by postsulfonation with chlorosulfonic acid. For most of the segmented copolymers, the degree of sulfonation was 100%. Polymers with high molecular weight were successfully obtained to give transparent, flexible, and tough membranes by solution casting. These novel segmented copolymer membranes showed well-developed phase separation. The copolymer 3 membranes showed proton conductivities over a range of relative humidity conditions that were comparable to Nafion and multiblock copolymers. Longer hydrophilic block length appeared to be effective in increasing proton diffusion coefficients, which coincide with the proton conductivity observations. The water uptake,

dimensional stability, and proton conductivity of the densely sulfonated segmented copolymers demonstrated that the strategy to combine segmented polymer architecture with high sulfonated blocks and pendent phenylsulfonic acid groups is a promising way to achieve high-performance PEM materials. Fuel-cell performance is under currently under investigation.

## AUTHOR INFORMATION

### Corresponding Author

\*E-mail: Michael.Guiver@nrc-cnrc.gc.ca (M.D.G.); ymlee@hanyang.ac.kr (Y.M.L.).

### Notes

<sup>†</sup>NRCC No. 52995.

## ACKNOWLEDGMENT

Funding for the project by the WCU program, National Research Foundation (NRF) of the Korean Ministry of Science and Technology (No. R31-2008-000-10092-0), is gratefully acknowledged.

## REFERENCES

- (1) Barbir, F. *PEM Fuel Cells: Theory and Practice*; Academic Press: New York, 2005; Chapter 10, pp 337–398.
- (2) Srinivasan, S. *Fuel Cells: From Fundamentals to Applications*; Springer: Heidelberg, 2006; Chapter 10, pp 575–605.
- (3) Jacobson, M. Z.; Colella, W. G.; Golden, D. M. *Science* **2005**, *308*, 1901–1905.
- (4) Roziere, J.; Jones, D. J. *Annu. Rev. Mater. Res.* **2003**, *33*, 503–555.
- (5) Lakshmanan, B.; Huang, W.; Olmeijer, D.; Weidner, J. W. *Electrochem. Solid-State Lett.* **2003**, *6*, A282–A285.
- (6) Mathias, M. F.; Makharia, R.; Gasteiger, H. A.; Conley, J. J.; Fuller, T. J.; Gittleman, C. J.; Kocha, S. S.; Miller, D. P.; Mittelsteadt, C. K.; Xie, T.; Yan, S. G.; Yu, P. T. *Interface* **2005**, *14*, 24.
- (7) Rikukawa, M.; Sanui, K. *Prog. Polym. Sci.* **2000**, *25*, 1463–1502.
- (8) Hickner, A. H.; Ghassemi, H.; Kim, Y. S.; Einsla, B. R.; McGrath, J. E. *Chem. Rev.* **2004**, *104*, 4587–4611.
- (9) Yin, Y.; Yamada, O.; Tanaka, K.; Okamoto, K. *Polym. J.* **2006**, *38*, 197–219.
- (10) Ghassemi, H.; McGrath, J. E.; Zawodzinski, T. A. *Polymer* **2006**, *47*, 4132–4139.
- (11) Bae, B.; Chiky, Y.; Miyatake, K.; Watanabe, M. *Macromolecules* **2010**, *43*, 2684–2691.
- (12) Kreuer, K. D. *J. Membr. Sci.* **2001**, *185*, 29–39.
- (13) Einsla, B. R.; McGrath, J. E. *Am. Chem. Soc. Div. Fuel Chem.* **2004**, *49*, 616–618.
- (14) Lafitte, B.; Puchner, M.; Jannasch, P. *Macromol. Rapid Commun.* **2005**, *26*, 1464–1469.
- (15) Lafitte, B.; Jannasch, P. *Adv. Funct. Mater.* **2007**, *17*, 2823–2834.
- (16) Liu, B.; Robertson, G. P.; Kim, D.-S.; Guiver, M. D.; Hu, W.; Jiang, Z. *Macromolecules* **2007**, *40*, 1934–1944.
- (17) Kim, Y. S.; Robertson, G. P.; Kim, Y. S.; Guiver, M. D. *Macromolecules* **2009**, *42*, 957–963.
- (18) Li, N.; Shin, D. W.; Hwang, D. S.; Lee, Y. M.; Guiver, M. D. *Macromolecules* **2010**, *43*, 9810–9820.
- (19) Lee, H. S.; Roy, A.; Lane, O.; Dunn, S.; McGrath, J. E. *Polymer* **2008**, *49*, 715–723.
- (20) Goto, K.; Rozhanskii, I.; Yamakawa, Y.; Otsuki, T.; Naito, Y. *Polym. J.* **2009**, *41*, 95–104.
- (21) Roy, A.; Yu, X.; Dunn, S.; McGrath, J. E. *J. Membr. Sci.* **2009**, *327*, 118–124.
- (22) Elabd, Y. A.; Hickner, M. A. *Macromolecules* **2011**, *44*, 1–11.
- (23) Einsla, M. L.; Kim, Y. S.; Hawley, M.; Lee, H. S.; McGrath, J. E.; Liu, B.; Guiver, M. D.; Pivovar, B. S. *Chem. Mater.* **2008**, *20*, 5636–5642.
- (24) Matsumura, S.; Hlil, A. R.; Lepiller, C.; Gaudet, J.; Guay, D.; Shi, Z.; Holdcroft, S.; Hay, A. S. *Macromolecules* **2008**, *41*, 281–284.
- (25) Matsumura, S.; Hlil, A. R.; Hay, A. S. *J. Polym. Sci., Part A: Polym. Chem.* **2008**, *46*, 6365–6375.
- (26) Matsumoto, K.; Higashihara, T.; Ueda, M. *Macromolecules* **2009**, *42*, 1161–1166.
- (27) De Araujo, C. C.; Kreuer, K. D.; Schuster, M.; Portale, G.; Mendil-Jakani, H.; Gebel, G.; Maier, J. *Phys. Chem. Chem. Phys.* **2009**, *11*, 3305–3312.
- (28) Schuster, M.; Araujo, C.; Atanasov, V.; Anderson, H.; Kreuer, K.; Maier, M. *Macromolecules* **2009**, *42*, 3129–3137.
- (29) Li, N.; Yasuda, T.; Cui, Z.; Zhang, S.; Li, S. J. *Polym. Sci., Part A: Polym. Chem.* **2008**, *46*, 2820–2832.
- (30) Li, N.; Liu, J.; Cui, Z.; Zhang, S.; Xing, W. *Polymer* **2009**, *50*, 4505–4511.
- (31) Bae, B.; Yoda, T.; Miyatake, K.; Uchida, H.; Watanabe, M. *Angew. Chem., Int. Ed.* **2010**, *49*, 317–320.
- (32) Nakabayashi, K.; Higashihara, T.; Ueda, M. *J. Polym. Sci., Part A: Polym. Chem.* **2010**, *48*, 2757–2764.
- (33) Nakabayashi, K.; Higashihara, T.; Ueda, M. *Macromolecules* **2010**, *43*, 5756–5761.
- (34) Takamuku, S.; Jannasch, P. *Macromol. Rapid Commun.* **2011**, *32*, 474–480.
- (35) Shin, C. K.; Maier, G.; Andreas, B.; Scherer, G. G. *J. Membr. Sci.* **2004**, *245*, 147–161.
- (36) Zhao, C.; Li, X.; Wang, Z.; Dou, Z.; Zhong, S.; Na, H. *J. Power Sources* **2006**, *280*, 643–650.
- (37) Zhao, C.; Lin, H.; Shao, K.; Li, X.; Ni, H.; Wang, Z.; Na, H. *J. Power Sources* **2006**, *162*, 1003–1009.
- (38) Noshay, A.; McGrath, J. E. *Block Copolymers: Overview and Critical Survey*; Academic Press: New York, 1977.
- (39) Kim, Y. S.; Einsla, B.; Sankir, M.; Harrison, W.; Pivovar, B. S. *Polymer* **2006**, *47*, 4026–4035.
- (40) Linkous, A.; Anderson, H. R.; Kopitzke, R. W.; Nelson, G. L. *Int. J. Hydrogen Energy* **1998**, *23*, 525–529.
- (41) Jia, L.; Xu, X.; Zhang, L.; Xu, J. *J. Appl. Polym. Sci.* **1996**, *60*, 1231–1237.